Exploring High-Purity Multiparton Scattering at Hadron Colliders

Jeppe R. Andersen,[1] Pier Francesco Monni,[2] Luca Rottoli,[3] Gavin P. Salam,[4,5] and Alba Soto-Ontoso[2]
[1]*Institute for Particle Physics Phenomenology, University of Durham, South Road, Durham DH1 3LE, United Kingdom*
[2]*CERN, Theoretical Physics Department, CH-1211 Geneva 23, Switzerland*
[3]*Physik Institut, Universität Zürich, CH-8057 Zürich, Switzerland*
[4]*Rudolf Peierls Centre for Theoretical Physics, Clarendon Laboratory, Parks Road, Oxford OX1 3PU, United Kingdom*
[5]*All Souls College, Oxford OX1 4AL, United Kingdom*

(Received 30 August 2023; revised 15 November 2023; accepted 30 November 2023; published 23 January 2024)

Multiparton interactions are a fascinating phenomenon that occur in almost every high-energy hadron-hadron collision yet are remarkably difficult to study quantitatively. In this Letter, we present a strategy to optimally disentangle multiparton interactions from the primary scattering in a collision. That strategy enables probes of multiparton interactions that are significantly beyond the state of the art, including their characteristic momentum scale, the interconnection between primary and secondary scatters, and the pattern of three and potentially even more simultaneous hard scatterings. This opens a path to powerful new constraints on multiparton interactions for LHC phenomenology and to the investigation of their rich field-theoretical structure.

DOI: 10.1103/PhysRevLett.132.041901

At high-energy hadron colliders such as CERN's Large Hadron Collider (LHC), almost every event that gets studied is accompanied by multiple additional parton interactions (MPI) from the same proton-proton collision; cf. Fig. 1. For example, in each proton-proton collision that produces a Z or Higgs boson (the "primary" process), models [1,2] suggest that there are about ten additional parton collisions that occur simultaneously, usually involving QCD scatterings of quarks and gluons. MPI are the subject of a rich array of studies, involving effects ranging from partonic correlations inside the proton to color reconnections between final-state quarks and gluons [3,4]. Their modeling is an essential component of every major simulation tool [5–7]. While often thought of as nonperturbative, we shall see clearly below that MPI involve transverse momenta of up to 10 GeV and beyond, i.e., close to the scale of many of the primary processes regularly studied at the LHC. In a context where there is an ambitious worldwide effort to bring high precision in perturbative QCD calculations for those primary process [8–10], our current partial understanding of MPI scatters risks becoming a limiting factor across much of the LHC program.

A major challenge in the experimental characterization of MPI is the difficulty of unambiguously separating the MPI signal from the primary hard scattering. In this Letter, we propose an approach to investigating MPI scatters in Drell-Yan events that optimally suppresses the contamination from the primary hard scattering. This opens the path to a program of experimental study of MPI that goes significantly beyond the current state of the art. Features that we will highlight include (a) the clarity of the MPI signal; (b) scope for quantitative investigations of the leading two hard scatters (2HS) that includes direct experimental

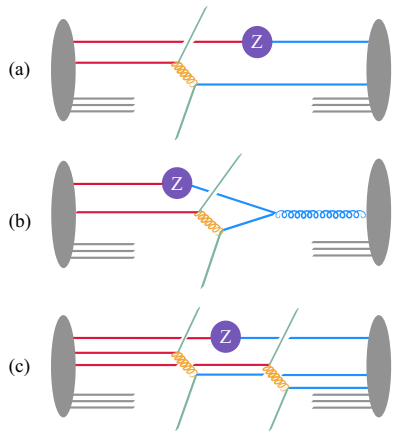

FIG. 1. Illustration of some MPI configurations that will be probed in this Letter: (a) standard double hard scattering, producing a Z boson and a pair of jets; (b) perturbative interconnection between the partons involved in the two hard scatterings, where the $\bar{q}$ that produces the Z and the q that scatters to produce the dijet system both have a common origin in the perturbative splitting of a gluon; and (c) a process with three hard scatterings.

sensitivity to perturbative interconnection [11–15] between the primary process and the second hard scatter—cf. Fig. 1(b); and (c) the potential for observation of high-purity triple parton scattering [Fig. 1(c)] [16,17] as well as sensitivity to even more than three scatters.

The foundation of our approach is the well-known fact [18] that if one considers events where the Drell-Yan pair has a low transverse momentum, the amount of initial-state radiation (ISR) is strongly constrained. To illustrate this quantitatively, we examine the average transverse momentum of the leading jet in Drell-Yan events as a function of the Z transverse momentum. Specifically, we consider $Z \to \mu^+\mu^-$ events and cluster all particles other than the muons with a jet algorithm (the anti-k_t algorithm [19] with a jet radius of $R = 0.7$, as implemented in FastJet [20]). Experimentally, this observable could be studied using charged-track jets (see below) or possibly standard jets in a dedicated low-pileup run. For now, to help expose the basic physical dynamics and scales, we retain all particles in the jet clustering. Figure 2 shows results both without and with MPI.

Let us first concentrate on the curves without MPI: One is from a resummed calculation (RadISH NNLL [21–23]), the other from a Monte Carlo simulation that uses a combination of MiNNLO [24,25] with POWHEG [26–28] and PYTHIA8.3 [5] (with HepMC2 [29]), and the third is from PYTHIA alone. All PYTHIA results use the Monash tune [30]. All three curves in Fig. 2 show the same features, namely, that for almost the whole range of p_{tZ} the average leading jet p_t is roughly proportional to p_{tZ} (with a proportionality coefficient close to 1), a consequence of momentum conservation between the jet and the Z boson. For p_{tZ} below about 2–3 GeV, the average leading jet p_t saturates. Events with very small p_{tZ} mostly occur when the transverse recoil from one initial-state radiated gluon cancels with that from other initial-state radiation. In this region, the average leading jet p_t has the parametric form ([31], Sec. A 1)

$$\langle p_{tj}^{\ell} \rangle_{p_{tZ}\to 0} \sim \Lambda \left(\frac{M}{\Lambda}\right)^{\kappa \ln[(2+\kappa)/(1+\kappa)]}, \qquad \kappa = \frac{2C_F}{\pi\beta_0}, \quad (1)$$

where Λ is the scale of the Landau pole in QCD, M is the invariant mass of the Drell-Yan pair, $\beta_0 = (11C_A - 2n_f)/(12\pi)$, and $C_F = 4/3$, $C_A = 3$, while n_f is the number of light quark flavors. With $n_f = 5$, this gives $\Lambda^{0.51} M^{0.49}$. In practice, this simple scaling is accurate only for large values of M, and the result from a full NNLL resummation (green curve) can be read off as the intercept of the corresponding curve in Fig. 2, i.e., 2.5 GeV, which coincides well with the intercept of the simulations without MPI (blue curves).

Next, consider the red curves in Fig. 2, those with MPI. For high p_{tZ} values, the leading jet p_t again tracks p_{tZ}. However, for low p_{tZ} values, the average leading jet p_t saturates at a value of about 10 GeV, which is significantly above the MPI-off result. The interpretation is that, in events with MPI, for low p_{tZ}, the leading jet almost always comes from an MPI scatter, not from the hard scatter, and it has a characteristic scale of the order of 10 GeV. This may be surprising if one thinks of MPI as genuinely non-perturbative, but less so if one considers that PYTHIA simulates MPI as semihard scatterings [1,2]. (We found similar results with the HERWIG7.2 [6,32] implementation of a comparable model [33,34].)

Figure 2 provides the foundation for the rest of this Letter. Specifically, if we consider events with a stringent cut on p_{tZ}, we ensure the near-total absence of hadronic radiation from the primary scatter (defined as that producing the Z). Existing experimental work confirms that the relative MPI contribution is enhanced by choosing a low p_{tZ} cut, for example, using $p_{tZ} < 5$ or 10 GeV [35–39]. From Fig. 2, we observe that if we choose a p_{tZ} cut that corresponds to the onset of the low p_{tZ} plateau of the MPI-off curves, i.e., $p_{tZ} < C_Z = 2$ GeV, we will obtain a near-optimal selection for the study of MPI: If one takes C_Z any higher, one increases contamination from hadronic activity due to the primary hard scatter; if one takes it any lower, there is no further advantage in terms of reducing primary hard-scatter contamination, but one loses cross section (and also reaches the limit of experimental lepton resolution). Our choice selects about 4%–5% of the Drell-Yan events that pass the muon cuts, i.e., a cross section after the C_Z cut of about 40 pb at $\sqrt{s} = 13.6$ TeV. For an LHC run 3 luminosity of 300 fb^{-1}, this would yield a sample of about 12 million events.

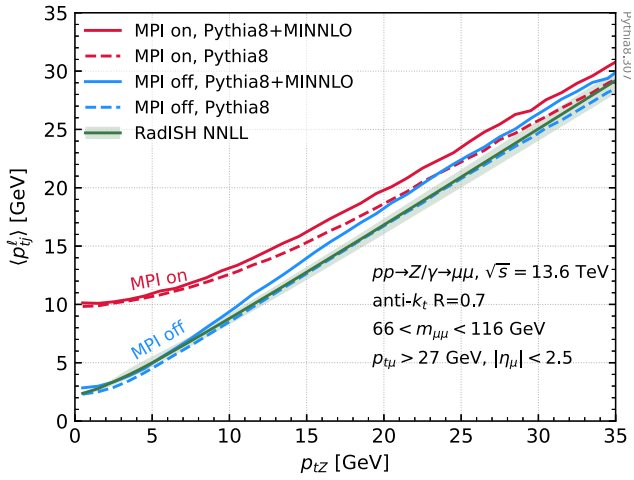

FIG. 2. The average leading jet transverse momentum $\langle p_{tj}^{\ell} \rangle$ as a function of the Z transverse momentum, in $Z \to \mu^+\mu^-$ events, with muon selection cuts as indicated in the plot. A radius of $R = 0.7$ is used here to reduce the loss of transverse momentum from the jet due to final-state radiation and hadronization and so more accurately track the transverse momentum of the underlying parton.

At first sight, Fig. 2 might suggest that MPI dynamics can be observed only at relatively low $p_{tj}^{\not\ell} \sim 10$ GeV. However, after applying the p_{tZ} cut, we can consider a much wider array of observables, some of which extend over a range of jet transverse momenta. The simplest is the cumulative inclusive jet spectrum, i.e., the average number of jets above some $p_{tj,\min}$, as a function of $p_{tj,\min}$:

$$\langle n(p_{tj,\min})\rangle_{C_Z} = \frac{1}{\sigma(p_{tZ} < C_Z)} \int_{p_{tj,\min}} dp_{tj} \frac{d\sigma_{\text{jet}}(p_{tZ} < C_Z)}{dp_{tj}}. \tag{2}$$

To a good approximation, this observable is given by a straight sum of the number of jets from the primary process and the number of jets from the MPI. The approximation is broken only by the potential overlap (in a cone of size R in rapidity and azimuth) of hadrons from the two scatters, and the approximation is exact in the limit of small R. Precisely for this reason, from here onward we shall use $R = 0.4$ rather than the $R = 0.7$ in Fig. 2. All results ($R = 0.4$ and $R = 0.7$) use area subtraction [40,41] to further reduce the impact of such overlap, notably as concerns any underlying-event pedestal of transverse momentum from the softest part of the MPI. We include a jet rapidity cut, $|y_j| < 2$, to mimic the central acceptance of the ATLAS and CMS detectors.

The cumulative inclusive jet spectrum is shown in Fig. 3. It is clear that the vast majority of jets come from the MPI scatters rather than the primary scatter, even for the relatively large value of $p_{tj,\min} = 50$ GeV. Looking instead at moderately low $p_{tj,\min}$ values, Fig. 3 indicates that on average there is one jet with $p_t \gtrsim 6$ GeV, which is broadly consistent with the plateau at 10 GeV in Fig. 2, considering

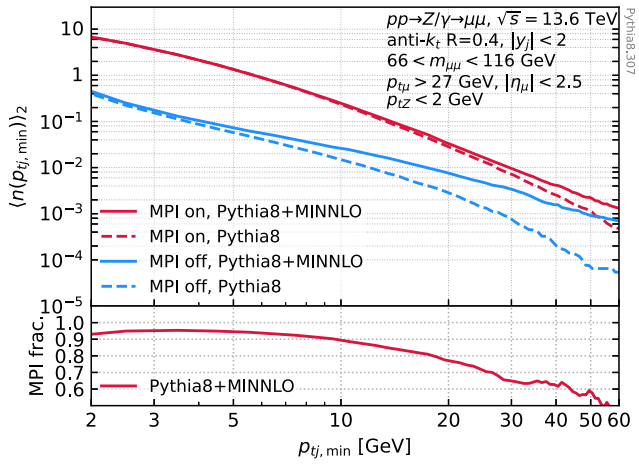

FIG. 3. The cumulative inclusive jet spectrum $\langle n(p_{tj,\min})\rangle_{C_Z}$ normalized to the number of events passing the cut $p_{tZ} < C_Z = 2$ GeV, with MPI on and off. The lower panel shows the fraction of jets that come from the MPI, demonstrating purity of 50%–90% across a broad range of $p_{tj,\min}$ jet cuts.

that Fig. 3 uses $R = 0.4$ instead of $R = 0.7$ and that it has a limited rapidity acceptance. Note that, for large $p_{tj,\min}$, the sample without MPI is dominated by events where the Z is accompanied by two opposing jets. The PYTHIA8+MiNNLO sample includes the matrix element for that process at leading order (LO), while PYTHIA8 does not, thus explaining the observed difference between the two curves for $p_t \gtrsim 10$ GeV.

It is useful to define the pure MPI contribution to the cumulative inclusive jet spectrum:

$$\langle n(p_{tj,\min})\rangle_{C_Z}^{\text{pure-MPI}} \equiv \langle n(p_{tj,\min})\rangle_{C_Z} - \langle n(p_{tj,\min})\rangle_{C_Z}^{\text{no-MPI}}. \tag{3}$$

In an actual experimental analysis, one might want to use a next-to-leading order (NLO) $Z + 2$ jet sample to subtract the hard-event contribution. Let us now see how Eq. (3) connects with the widely used "pocket formula" for double-parton scattering. That formula states that the double-parton scattering cross section for two hard processes A and B is given by

$$\sigma_{AB} = \frac{\sigma_A \sigma_B}{\sigma_{\text{eff}}}, \tag{4}$$

where σ_{eff} for pp collisions is measured to be of the order of 15–20 mb [42–48] (for processes involving a vector boson) and is related to an effective area over which interacting partons are distributed in the proton. We take process A to be Z production with $p_{tZ} < C_Z$ and process B to be inclusive jet production and consider a $p_{tj,\min}$ that is large enough for the pocket formula to be valid, i.e., such that $\sigma_B/\sigma_{\text{eff}} \ll 1$. This yields ([31], Sec. A 2)

$$\langle n(p_{tj,\min})\rangle_{C_Z}^{\text{pure-MPI}} \simeq \frac{1}{\sigma_{\text{eff}}} \int_{p_{tj,\min}} dp_{tj} \frac{d\sigma_{\text{jet}}}{dp_{tj}}, \tag{5}$$

where $(d\sigma_{\text{jet}}/dp_{tj})$ is the inclusive jet cross section for jet production, without any requirement that a Z be present in the event. (Using the PYTHIA minimum-bias process to generate the reference jet sample, we find $\sigma_{\text{eff}} \simeq 30$ mb, somewhat larger than in standard measurements. This may imply that PYTHIA is underestimating the MPI or overestimating the minimum-bias jet spectrum or that the data used for standard σ_{eff} extractions have a higher level of MPI activity than would be seen with a $p_{tZ} < 2$ GeV cut.) The right-hand side of Eq. (5) does not involve C_Z, and, thus, the pocket-formula prediction is that $\langle n(p_{tj,\min})\rangle_{C_Z}^{\text{pure-MPI}}$ should be independent of C_Z.

The pocket formula is, however, known to be an approximation. The difficulty of obtaining a pure MPI sample has so far limited the scope for investigating more sophisticated theoretical predictions. One particularly interesting effect not captured in the pocket formula relates to

perturbative interconnection between the primary scattering and the secondary scattering, as in Fig. 1(b), where at least some of the partons entering the two separate hard scattering processes (Z and dijet production) have a common origin, e.g., a perturbative $g \to q\bar{q}$ splitting, with the $\bar{q}$ involved in Z production and the q involved in dijet production.

Our procedure of constraining the Z transverse momentum means that the partons that annihilate to produce the Z will almost always have a low transverse momentum, which reduces the likelihood of their having been produced in a perturbative splitting. In contrast, if we relax the constraint on p_{tZ}, we will allow for substantially more initial-state radiation from the partons that go on to produce the Z. The ISR partons can then take part in a separate hard scatter, i.e., increasing the interconnection contribution to 2HS [Fig. 1(b)].

To evaluate potential sensitivity to this effect, we examine the ratio between the 2HS rate with loose ($C_Z = 15$ GeV) and tight ($C_Z = 2$ GeV) constraints on p_{tZ}:

$$r_{15/2} = \frac{\langle n(p_{tj,\min})\rangle_{15}^{\text{pure-MPI}}}{\langle n(p_{tj,\min})\rangle_{2}^{\text{pure-MPI}}}. \tag{6}$$

In each case, the 2HS rate is normalized to the number of Z bosons that pass the selection cut. With the pocket formula the ratio should be 1, and so an experimental measurement of $r_{15/2}$ has the potential to provide powerful constraints on deviations from the pocket formula. Note that, with $C_Z = 15$ GeV, the pure-MPI jet fraction is predicted by PYTHIA8+MiNNLO to be about 25% at $p_{tj,\min} = 40$ GeV ([31], Sec. A 3), which should be adequate for a quantitative extraction of $r_{15/2}$.

Figure 4 shows the $r_{15/2}$ ratio evaluated in three ways. The PYTHIA8+MiNNLO curve corresponds to a full analysis, using PYTHIA8+MiNNLO curve itself (without MPI), to evaluate the no-MPI contribution for Eq. (3). PYTHIA8 does not include a perturbative interconnection mechanism (though it has correlations related to momentum conservation and color reconnections [49]), and one sees a result consistent with $r_{15/2} = 1$ to within statistical fluctuations.

Figure 4 also includes curves from the dShower program [50,51]. This is a state-of-the-art code that simulates a pure 2HS component, with the option of including interconnection effects according to Ref. [15]. Rather than carrying out a full analysis (which would require a consistent merging with a 1HS component), we determine the $r_{15/2}$ ratio based on the truth Monte Carlo information about the transverse momentum of the hard outgoing partons in the $2 \to 2$ interaction, i.e., the second hard scattering. The pink curve is the result without interconnection (with MSTW2008 PDFs (parton distribution functions) [52]) and is consistent with 1. The orange curve includes interconnection effects, and one clearly sees a 25%–30% violation of the pocket formula. The scope for measuring this experimentally in a full analysis depends critically on the systematic errors associated with the subtraction of the no-MPI contribution in Eq. (3). The significance of such a signal is discussed in [31], Sec. A 3, for various scenarios of uncertainties on the no-MPI term, and the conclusion is that reasonable assumptions lead to at least 2 standard deviations at low $p_{tj,\min}$, which would correspond to exclusion of the pocket formula. The significance can be raised by increasing the accuracy of the no-MPI predictions, e.g., with improved higher-order calculations.

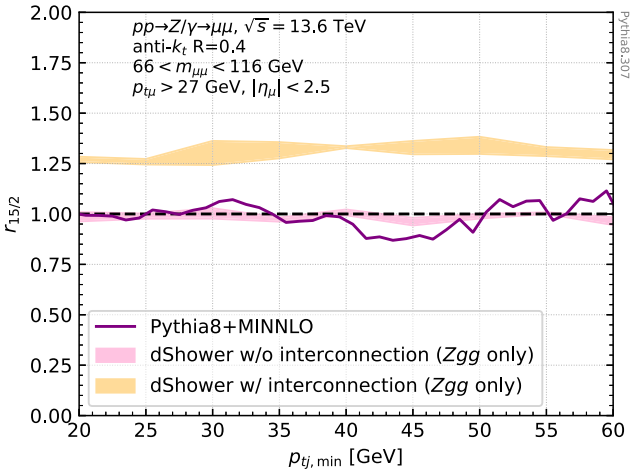

FIG. 4. PYTHIA8+MiNNLO and dshower results for the $r_{15/2}$ ratio in Eq. (6). Note the deviation from 1 when perturbative interconnection is turned on between the primary and secondary hard scatters, i.e., diagrams as in Fig. 1(b). The dshower bands correspond to scale variation (see [31], Sec. A 3 for further details). They include only the Zgg final state, which represents about 50% of independent 2HS, and so should be taken as qualitative. No jet rapidity cut is applied.

The final question that we turn to is the sensitivity to more than two simultaneous perturbative scatterings. So far, the only attempt to study this experimentally has been in triple charmonium production, where the measured cross section has a large uncertainty [17,53] and where generic difficulties in understanding charmonium production complicate the interpretation of the results.

Here, we propose the study of charged-track jets, with moderately low p_t cuts. To illustrate the study, we construct charged-track jets using charged particles with $|\eta| < 2.4$ and $p_t > 0.5$ GeV. The use of charged particles enables the study of moderately low p_t jets even in high-pileup runs, thus exploiting the full luminosity of the LHC. We order the jets in decreasing p_t and first study the two leading jets, with a "product" cut [54] $\sqrt{p_{t1}p_{t2}} > 9 f_{\text{chg}}$ GeV and a ratio cut $p_{t2} > 0.6 p_{t1}$. We quote the cuts in terms of a charged-to-neutral conversion ratio $f_{\text{chg}} = 0.65$. The overall scale of the cuts ensures a non-negligible likelihood that each event contains at least one pair of jets.

Figure 5 shows results for the absolute difference in azimuthal angles between the two jets, $\Delta\phi_{12}$.

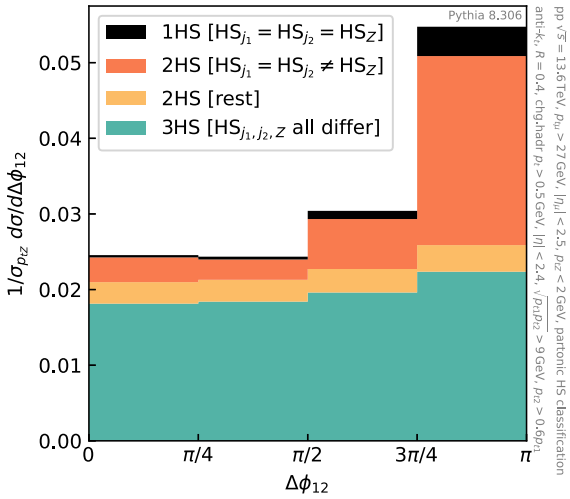

FIG. 5. The distribution of the absolute value of $\Delta\phi_{12}$ between the two leading charged-track jets in events with $p_{tZ} < 2$ GeV (cf. the text for jet cuts). The plot shows a clear signal not just of 2HS (in the peak) but also of 3HS (plateau).

This observable is expected to peak around $\Delta\phi_{12} = \pi$ when the two jets come from the same hard partonic interaction and to be uniformly distributed between 0 and π when the two jets come from distinct partonic interactions. The plot clearly shows both a peak and a continuum component. A parton-level-based decomposition ([31], Sec. A 5) of each histogram bin shows that the plateau is dominated by events with three hard scatterings (3HS), where each of the two leading jets comes from a different HS (each distinct from the one that produced the Z). The enhancement near $\Delta\phi_{12} = \pi$ originates mostly from 2HS where the two jets are from a single HS that is distinct from the one that produced the Z; cf. Fig. 1(a). A measurement of $\Delta\phi_{12}$ would, therefore, provide clear and quantifiable indications not only of 2HS, but also of 3HS.

With such an unambiguous signal of 3HS, one may wonder if it is possible to gain even further insight. One obvious question is whether one can identify a system with two back-to-back jets from one hard interaction and two further back-to-back jets from another hard interaction, all distinct from the Z hard interaction; cf. Fig. 1(c). This appears to be on the edge of feasibility but also brings sensitivity to 4HS ([31], Sec. A 4).

In conclusion, the study of Drell-Yan events with a tight cut on p_{tZ} opens the door to numerous new studies of multiparton interactions, with high-purity 2HS samples, sensitivity to the perturbative quantum field theory effects that interconnect primary and secondary scatters, and the scope for extensive investigations into 3HS and perhaps even beyond. The studies outlined here are all possible with existing and run 3 data. The subset of studies that extends to relatively low jet p_t values should be feasible with charged-track jets. There is also ample scope for further exploration, for example, in terms of the choices of jet cuts or studies in other collision systems such as p-Pb. We expect experimental results on these questions to have the potential for a significant impact not just on our intrinsic understanding of multiparton interactions, but also for the accurate modeling of hadron collisions that will be needed for the broad range of high-precision physics that will be carried out at the high-luminosity upgrade of the LHC and at potential future hadron colliders.

We are grateful to Jonathan Gaunt for extensive discussions and access to the dShower code and to Lucian Harland-Lang and Paolo Torrielli for discussions in the early stages of this work. The work of J. R. A. is supported by the STFC under Grant No. ST/P001246/1. The work of P. F. M. has been funded by the European Union (ERC, Grant Agreement No. 101044599, JANUS). The work of L. R. is supported by the Swiss National Science Foundation Contract No. PZ00P2_201878. The work of G. P. S. and A. S.-O. has been funded by the European Research Council (ERC) under the European Union's Horizon 2020 research and innovation program (Grant Agreement No. 788223), and that of G. P. S. additionally by a Royal Society Research Professorship (RP\R1\180112) and by the Science and Technology Facilities Council (STFC) under Grant No. ST/T000864/1. This research was supported by the Munich Institute for Astro-, Particle and BioPhysics (MIAPbP) which is funded by the Deutsche Forschungsgemeinschaft (DFG, German Research Foundation) under Germany's Excellence Strategy—EXC-2094-390783311. Views and opinions expressed are those of the authors only and do not necessarily reflect those of the European Union or the European Research Council Executive Agency. Neither the European Union nor the granting authority can be held responsible for them.

[1] T. Sjostrand and M. van Zijl, Phys. Rev. D **36**, 2019 (1987).
[2] T. Sjostrand and P. Z. Skands, J. High Energy Phys. 03 (2004) 053.
[3] *Proceedings of the 7th International Workshop on Multiple Partonic Interactions at the LHC (MPI@LHC 2015): Miramare, Trieste, Italy, 2015*, edited by H. Jung, D. Treleani, M. Strikman, and N. van Buuren (2016).
[4] *Multiple Parton Interactions at the LHC*, edited by P. Bartalini and J. R. Gaunt (World Scientific, Singapore, 2019), Vol. 29.
[5] C. Bierlich *et al.*, SciPost Phys. Codebases 8 (2022)..
[6] J. Bellm *et al.*, Eur. Phys. J. C **80**, 452 (2020).
[7] E. Bothmann *et al.* (Sherpa Collaboration), SciPost Phys. **7**, 034 (2019).
[8] A. Huss, J. Huston, S. Jones, and M. Pellen, J. Phys. G **50**, 043001 (2023).
[9] F. Caola, W. Chen, C. Duhr, X. Liu, B. Mistlberger, F. Petriello, G. Vita, and S. Weinzierl, in Proceedings of Snowmass 2021 (2022); arXiv:2203.06730.
[10] J. M. Campbell *et al.*, in Proceedings of Snowmass 2021 (2022); arXiv:2203.11110.

[11] M. Diehl and A. Schafer, Phys. Lett. B **698**, 389 (2011).
[12] B. Blok, Y. Dokshitser, L. Frankfurt, and M. Strikman, Eur. Phys. J. C **72**, 1963 (2012).
[13] M. Diehl, D. Ostermeier, and A. Schafer, J. High Energy Phys. 03 (2012) 089; 03 (2016) 001(E).
[14] B. Blok, Y. Dokshitzer, L. Frankfurt, and M. Strikman, Eur. Phys. J. C **74**, 2926 (2014).
[15] M. Diehl, J. R. Gaunt, and K. Schönwald, J. High Energy Phys. 06 (2017) 083.
[16] D. d'Enterria and A. M. Snigirev, Phys. Rev. Lett. **118**, 122001 (2017).
[17] A. Tumasyan *et al.* (CMS Collaboration), Nat. Phys. **19**, 338 (2023).
[18] G. Parisi and R. Petronzio, Nucl. Phys. **B154**, 427 (1979).
[19] M. Cacciari, G. P. Salam, and G. Soyez, J. High Energy Phys. 04 (2008) 063.
[20] M. Cacciari, G. P. Salam, and G. Soyez, Eur. Phys. J. C **72**, 1896 (2012).
[21] P. F. Monni, E. Re, and P. Torrielli, Phys. Rev. Lett. **116**, 242001 (2016).
[22] W. Bizon, P. F. Monni, E. Re, L. Rottoli, and P. Torrielli, J. High Energy Phys. 02 (2018) 108.
[23] P. F. Monni, L. Rottoli, and P. Torrielli, Phys. Rev. Lett. **124**, 252001 (2020).
[24] P. F. Monni, P. Nason, E. Re, M. Wiesemann, and G. Zanderighi, J. High Energy Phys. 05 (2020) 143; 02 (2022) 031(E).
[25] P. F. Monni, E. Re, and M. Wiesemann, Eur. Phys. J. C **80**, 1075 (2020).
[26] P. Nason, J. High Energy Phys. 11 (2004) 040.
[27] S. Frixione, P. Nason, and C. Oleari, J. High Energy Phys. 11 (2007) 070.
[28] S. Alioli, P. Nason, C. Oleari, and E. Re, J. High Energy Phys. 06 (2010) 043.
[29] M. Dobbs and J. B. Hansen, Comput. Phys. Commun. **134**, 41 (2001).
[30] P. Skands, S. Carrazza, and J. Rojo, Eur. Phys. J. C **74**, 3024 (2014).
[31] See Supplemental Material at http://link.aps.org/supplemental/10.1103/PhysRevLett.132.041901 for further technical details.
[32] G. Bewick, S. Ferrario Ravasio, P. Richardson, and M. H. Seymour, J. High Energy Phys. 04 (2020) 019.
[33] M. Bahr, S. Gieseke, and M. H. Seymour, J. High Energy Phys. 07 (2008) 076.
[34] J. Bellm, S. Gieseke, and P. Kirchgaesser, Eur. Phys. J. C **80**, 469 (2020).
[35] CMS Collaboration, Eur. Phys. J. C **83**, 722 (2023).
[36] A. M. Sirunyan *et al.* (CMS Collaboration), J. High Energy Phys. 07 (2018) 032.
[37] S. Alioli, C. W. Bauer, S. Guns, and F. J. Tackmann, Eur. Phys. J. C **76**, 614 (2016).
[38] R. Kumar, M. Bansal, S. Bansal, and J. B. Singh, Phys. Rev. D **93**, 054019 (2016).
[39] G. Aad *et al.* (ATLAS Collaboration), Eur. Phys. J. C **74**, 3195 (2014).
[40] M. Cacciari and G. P. Salam, Phys. Lett. B **659**, 119 (2008).
[41] M. Cacciari, G. P. Salam, and G. Soyez, J. High Energy Phys. 04 (2008) 005.
[42] F. Abe *et al.* (CDF Collaboration), Phys. Rev. Lett. **79**, 584 (1997).
[43] V. M. Abazov *et al.* (D0 Collaboration), Phys. Rev. D **81**, 052012 (2010).
[44] G. Aad *et al.* (ATLAS Collaboration), New J. Phys. **15**, 033038 (2013).
[45] S. Chatrchyan *et al.* (CMS Collaboration), J. High Energy Phys. 03 (2014) 032.
[46] M. Aaboud *et al.* (ATLAS Collaboration), Phys. Lett. B **790**, 595 (2019).
[47] A. Tumasyan *et al.* (CMS Collaboration), J. High Energy Phys. 01 (2022) 177.
[48] CMS Collaboration, Phys. Rev. Lett. **131**, 091803 (2023).
[49] J. R. Christiansen and P. Z. Skands, J. High Energy Phys. 08 (2015) 003.
[50] B. Cabouat, J. R. Gaunt, and K. Ostrolenk, J. High Energy Phys. 11 (2019) 061.
[51] B. Cabouat and J. R. Gaunt, J. High Energy Phys. 10 (2020) 012.
[52] A. D. Martin, W. J. Stirling, R. S. Thorne, and G. Watt, Eur. Phys. J. C **70**, 51 (2010).
[53] J. Gaunt, Nat. Phys. **19**, 305 (2023).
[54] G. P. Salam and E. Slade, J. High Energy Phys. 11 (2021) 220.